NeuroImage: Clinical 28 (2020) 102480

Contents lists available at ScienceDirect

NeuroImage: Clinical

journal homepage: www.elsevier.com/locate/ynicl

Topological reorganization of brain functional networks in patients with mitochondrial encephalomyopathy with lactic acidosis and stroke-like episodes

Rong Wang [a,b,c,1], Jie Lin [d,1], Chong Sun [d], Bin Hu [a,c], Xueling Liu [a,c], Daoying Geng [a,b,c], Yuxin Li [a,c,*], Liqin Yang [a,c,*]

[a] Department of Radiology, HuaShan Hospital, Fudan University, Shanghai 200040, China
[b] Shanghai Institution of Medical Imaging, Shanghai 200032, China
[c] Institute of Functional and Molecular Medical Imaging, Fudan University, Shanghai 200040, China
[d] Department of Neurology, Huashan Hospital, Fudan University, Shanghai 200040, China

ARTICLE INFO

Keywords:
MELAS
Resting state
Graph theory analysis
Brain functional networks

ABSTRACT

Mitochondrial encephalomyopathy with lactic acidosis and stroke-like episodes (MELAS) is a rare maternally inherited genetic disease; however, little is known about its underlying brain basis. Furthermore, the topological organization of brain functional network in MELAS has not been explored. Here, 45 patients with MELAS (22 at acute stage, 23 at chronic stage) and 22 normal controls were studied using resting- state functional magnetic resonance imaging and graph theory analysis approaches. Topological properties of brain functional networks including global and nodal metrics, rich club organization and modularity were analyzed. At the global level, MELAS patients exhibited reduced clustering coefficient, normalized clustering coefficient, normalized characteristic path length and local network efficiency compared with the controls. At the nodal level, several nodes with abnormal degree centrality and nodal efficiency were detected in MELAS patients, and the distribution of these nodes was partly consistent with the stroke-like lesions. For rich club organization, rich club nodes were reorganized and the connections among them were decreased in MELAS patients. Modularity analysis revealed that MELAS patents had altered intra- or inter-modular connections in default mode network, fronto-parietal network, sensorimotor network, occipital network and cerebellum network. Notably, the patients at acute stage showed more obvious changes in these topological properties than the patients at chronic stage. These findings indicated that MELAS patients, particularly those at acute stage, exhibited topological reorganization of the whole-brain functional network. This study may help us to understand the neuropathological mechanisms of MELAS.

1. Introduction

Mitochondrial encephalomyopathy with lactic acidosis and stroke-like episodes (MELAS), the most common type of mitochondrial disease, is a rare maternally inherited genetic disease mostly affecting children and young adults (Pavlakis et al., 1984). The molecular basis of MELAS is m.3243A > G mutation in the MT-TL1 gene encoding $tRNA^{Leu(UUR)}$ (Goto et al., 1990). Without an effective pharmaceutical or dietary intervention, MELAS often leads to disability or even early death. The symptoms of MELAS include easy fatigability, endocrinopathies, gastrointestinal dysmotility, diabetes mellitus, dementia, growth retardation and stroke-like episodes (SLEs) (Koenig et al., 2016). SLEs are the cardinal features of MELAS, which commonly present headaches, seizures, hearing loss, cortical blindness, aphasia and motor weakness (El-Hattab et al., 2015). In MELAS, recurrent SLEs followed by symptomatic remission may progressively damage the brain and cause neurological and neuropsychological deficits (Kaufmann et al., 2011). The most common neuropathological findings during the chronic stage of MELAS are foci of necrosis and peculiar vascular changes (Ito et al., 2011). Concerning the neuropathology of the acute stage of MELAS, autopsy

* Corresponding authors: Department of Radiology, HuaShan Hospital Institute of Functional and Molecular Medical Imaging, Fudan University, 12 Middle Wulumuqizhong Road, Shanghai 200040, China.
E-mail addresses: liyuxin@fudan.edu.cn (Y. Li), mozi001_ren@sina.com (L. Yang).
[1] Co-First author: Rong Wang and Jie Lin contribute equally to this study.

https://doi.org/10.1016/j.nicl.2020.102480
Received 30 June 2020; Received in revised form 16 October 2020; Accepted 19 October 2020
Available online 27 October 2020

specimen showed extensive petechial hemorrhage along the gyri of the cortex in the acute stroke-likes lesions (Iizuka et al., 2002). Stroke-like lesions (SLLs) are the characteristics showing on magnetic resonance imaging (MRI) images in MELAS patients (Malhotra and Liebeskind, 2016). Typical MRI findings in an SLL of MELAS include gyral swelling, gyriform cortical diffusion restriction and subcortical white matter T2 fluid-attenuated inversion recovery (FLAIR) hyperintensity (Bhatia et al., 2020). Furthermore, recent studies have demonstrated the different features on neuroimaging between acute stage and chronic stage, such as the alterations of cerebral diffusion, perfusion and metabolism in SLLs (Bhatia et al., 2020; Hongo et al., 2019; Lee et al., 2018; Li et al., 2019; Xu et al., 2018). However, the characteristics of acute and chronic stages remains largely unknown, and the neuropathological mechanisms of MELAS need to be further explored.

Resting-state functional MRI (rs-fMRI) is a powerful neuroimaging technique that can noninvasively measure spontaneous activity in human brain (Biswal et al., 1995). Rs-fMRI has been widely used to study functional connectivity patterns in healthy and diseased populations, such as attention-deficit/hyperactivity disorder (Sudre et al., 2017), major depressive disorder (Albert et al., 2019) and bipolar disorder (Syan et al., 2018). Until now, no study has reported the changes of functional connectivity in MELAS. Graph theory is an advanced approach to investigate the complex network of human brain connectome (Bullmore and Sporns, 2009; He and Evans, 2010). With the aid of graph theory analysis, rs-fMRI studies have shown that the human brain functional networks exhibit many important topological properties, such as small-world properties for balanced functional segregation and integration, modular structure, rich-club organization and densely connected hubs. Recent studies have revealed the disrupted topological properties of functional network in several neurological diseases (e.g. Alzheimer disease, Parkinson disease, stroke, etc.) (Adhikari et al., 2017; Göttlich et al., 2013; Tijms et al., 2013), providing novel insights into the neuropathological mechanism of brain injury in disease state. Stroke-like lesions (SLLs) are common radiological findings in patients with MELAS. A prior study reported that brain lesion, such as tumor, stroke and traumatic brain injury, could lead to the disturbances in network organization (Aerts et al., 2016). However, in MELAS, how the topology of brain functional network changes and whether these changes are related to the distribution of SLLs have not been studied yet.

Therefore, in this study, we applied rs-fMRI with graph theory analysis to explore the topological organization of whole-brain functional networks in patients with MELAS at acute and chronic stages. Here, we hypothesized that MELAS patients, especially those at acute stage, would exhibit topological disturbance and reorganization in the whole brain, and this effect might be related with the distributions of SLLs.

2. Materials and methods

2.1. Subjects

The study was approved by the Institutional Review Board of Huashan Hospital and was conducted in accordance with the tenets of the Declaration of Helsinki. Written informed consent was obtained from all participants.

All patients were examined by a specialized expert with 15 years' experience in MELAS. The diagnosis of MELAS was based on clinical manifestation, MRI, muscle biopsy and genetic testing (Yatsuga et al., 2012). Specifically, only MELAS patients carrying m.3243A > G mutation were included in this study. Twenty-five patients at acute stage (MELAS-acute group, within 1 week after the stroke-like episodes, 12 males, 10 females; mean age, 25.7 ± 8.8 years) and 25 patients who were free from SLEs symptoms at chronic stage (MELAS-chronic group, within 6–8 months after stroke-like episodes, 12 males, 11 females; mean age, 29.2 ± 11.3 years) were enrolled in this study from June 2015 to November 2019. In addition, 22 normal control (NC) volunteers (10 males, 12 females; mean age, 29.1 ± 6.9 years) who were age and gender matched were recruited for this study.

The exclusion criteria for all subjects included any history or suspicion of psychiatric or neurological diseases except for MELAS (i.e. Parkinson's disease, autism, multiple sclerosis, depressive disorder, etc), tumors, head injury, dementia and contraindications for MRI examinations.

2.2. MRI acquisition

MRI was performed on a 3.0 Tesla scanner (Discovery MR750, General Electric, Boston, MA, USA) equipped with an 8-channel head coil. During MRI scanning, all subjects were instructed to keep their eyes closed but not to fall asleep. The rs-fMRI images were obtained using a single-shot gradient-recalled echo planar imaging (EPI) sequence with the following parameters: repetition time (TR) = 2000 ms, echo time (TE) = 30 ms, slice thickness = 4 mm, flip angle = 90°, slices = 35, field of view (FOV) = 240 mm × 240 mm, matrix size = 64 × 64, No. of volumes = 210. The high-resolution 3D T1-weighted images were acquired by a brain volume (BRAVO) sequence: TR = 8.2 ms, TE = 3.2 ms, slice thickness = 1.2 mm, flip angle = 12°, slices = 170, FOV = 240 mm × 240 mm, matrix size = 256 × 256. T2-weighted fluid-attenuated inversion recovery (FLAIR) scans were acquired with the following parameters: TR = 8800 ms, TE = 145 ms, slice thickness = 6 mm, slices = 18, FOV = 240 mm × 240 mm, matrix size = 224 × 224.

2.3. Data preprocessing

The rs-fMRI images were preprocessed using MATLAB 2016a (MathWorks, Natick, MA, USA) and DPABI toolbox (http://rfmri.org/dpabi) (Yan et al., 2016). For each subject, the first 10 volumes of the rs-fMRI dataset were removed for magnetization stabilization, leaving 200 volumes for further analysis. The remaining volumes received a slice timing correction according to the acquisition time differences between slices. The volumes were then spatial realigned to correct for head motion. The mean frame-wise displacement (FD) was calculated, which represents head movement (Power et al., 2014). Subjects with a head motion > 2.5 mm translation or a 2.5° rotation or 0.25 FD were excluded (MELAS-acute = 3, MELAS-chronic = 2). Thus, after excluding these subjects, the final sample comprised of 67 subjects (MELAS-acute = 22, MELAS-chronic = 23, NC = 22). Several nuisance variables including Friston's 24 parameters (Friston et al., 1996) of head motion, the signals from white matter and cerebrospinal fluid were regressed out. Because global signal regression may introduce artificial negative correlations in the functional network (Fox et al., 2009; Murphy et al., 2009) and global signals may also contain important information (Yang et al., 2014), the global signals were not regressed out in the present study. Then, the images were normalized to standard Montreal Neurological Institute (MNI) space by resampling voxel size to 3 mm × 3 mm × 3 mm through DARTEL approach. Next, the images were spatially smoothed by using a Gaussian kernel with full-width at half-maximum (FWHM) of 6 mm. Finally, the time series was filtered between 0.01 and 0.08 Hz to reduce the effects of high-frequency physiological noises.

2.4. Functional network construction

The functional network was constructed and analyzed using GRETNA toolbox (http://www.nitrc.org/projects/gretna/) (Wang et al., 2015) and the results were visualized using BrainNet Viewer software (https://www.nitrc.org/projects/bnv/) (Xia et al., 2013). In graph theory, a network is represented as nodes that are connected by edges. A node is a brain region, and an edge is present when there is an anatomical connection or functional correlation between two nodes. We constructed the brain functional network for each subject according to the Dos-160 template, which consists of 160 regions of interest (ROIs)

(Dosenbach et al., 2010). This template is regarded as an optimal template for constructing brain functional networks (Yao et al., 2015). The 160 ROIs in Dos-160 template are classified into 6 functional subnetworks, including the default mode network (DMN), fronto-parietal network (FPN), cingulo-opercular network (CON), sensorimotor network (SMN), occipital network (ON), and cerebellum network (CN) (Fig. 1a). The names and the abbreviations of these ROIs were listed in Table S1 (supplementary materials).

For each subject, the time series for each ROI, which is already extracted as spheres of 5 mm radius from the Dos-160 template, were extracted by averaging the time courses of all the voxels within a ROI. Next, Pearson's linear correlation was calculated between the mean time series of each ROI. Considering the ambiguous biological explanation of negative correlation (Fox et al., 2009; Murphy et al., 2009; Weissenbacher et al., 2009), we restricted our analysis to positive correlation connections and set the negative correlation coefficients as zero. Then, Fisher's r-to-z transformation was performed to translate the correlation matrix to improve normality. Finally, the correlation matrix was binarized, resulting an undirected and unweighted 160 × 160 symmetric positive correlation matrix for each subject. Here, network sparsity threshold was selected as S = 15%, which maintained the high connectedness of the brain networks and simultaneously removed as many spurious correlations as possible.

2.5. Network analysis

2.5.1. Global and nodal metrics

For the brain networks at each sparsity threshold, we calculated global network metrics, which comprise: 1) small-world properties including clustering coefficient (Cp), characteristic path length (Lp), normalized clustering coefficient (γ), normalized characteristic path length (λ), and small-worldness (σ); 2) network efficiency including global network efficiency (E_{glob}) and local network efficiency (E_{loc}). High Cp, γ, and E_{loc} can show functional segregation of brain network, which is the ability for specialized neuronal processing; Low Lp, λ, and high E_{glob} can reflect the functional integration in the brain, which is the ability for global information communication; σ characterizes an optimized balance between network segregation and integration (Dai et al., 2019). Typically, a small-world network satisfies the following criteria: $\gamma > 1$ and $\lambda \approx 1$, or $\sigma > 1$ (Uehara et al., 2014). In addition, to explore nodal properties of brain functional network, degree centrality (DC) and nodal efficiency (E_{nodal}) were calculated. DC is defined as the number of connections upon a node. E_{nodal} quantifies the ability of a node in communication transfer within a network. The comprehensive description of these network metrics can be found in prior review article (Rubinov and Sporns, 2010).

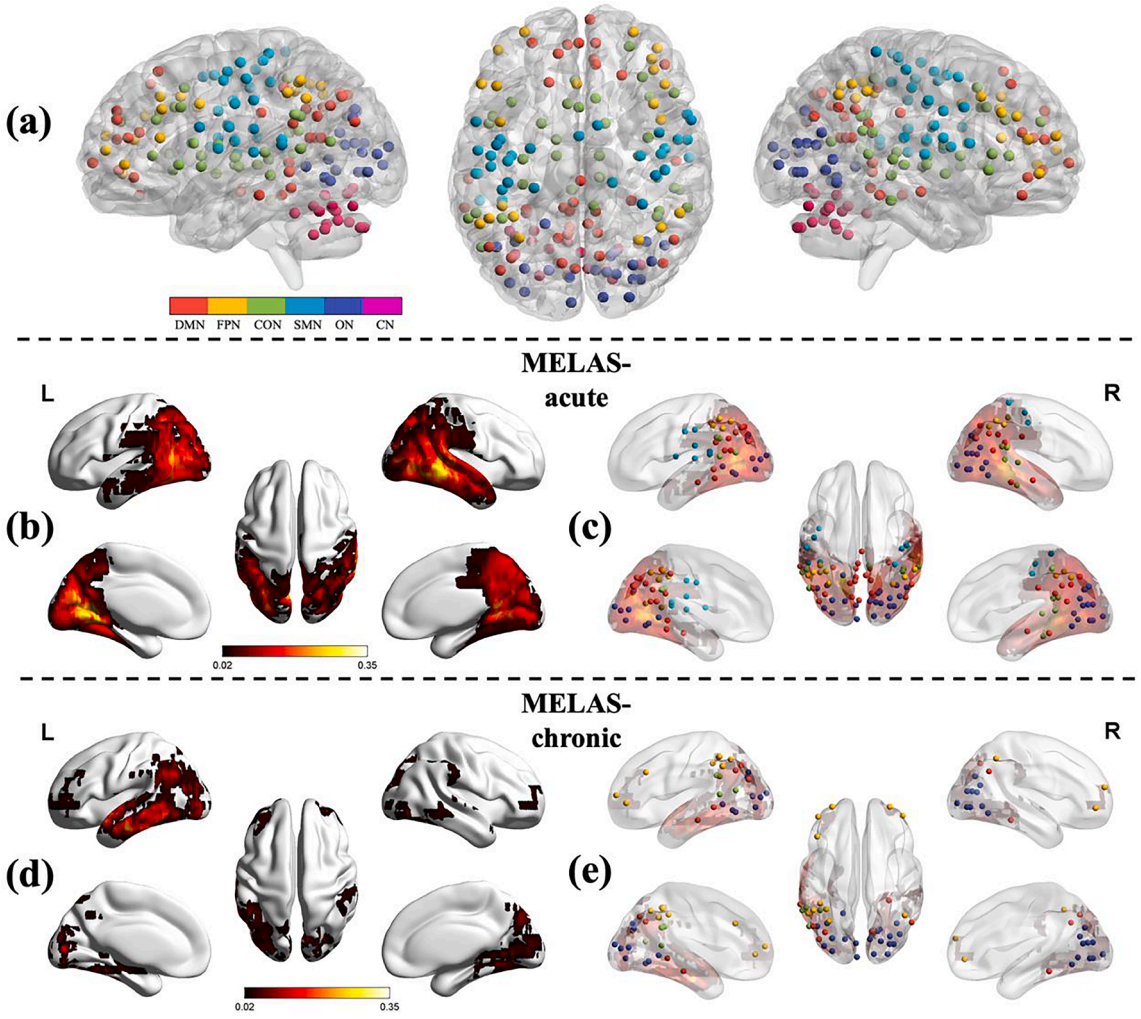

Fig. 1. The regions of interest in the Dos-160 template (a). The colors of nodes represented the different modules of brain functional networks. DMN: the default mode network; FPN: the fronto-parietal network; CON: the cingulo-opercular network; SMN: the sensorimotor network; ON: the occipital network; CN: the cerebellum network. Stroke-like lesions probability map in MELAS-acute (b) and MELAS-chronic (d) groups. The color bar represents the frequency of lesions in each voxel. Stroke-like lesions overlapped with the nodes of the Dos-160 template in MELAS-acute (c) and MELAS-chronic (e) groups.

2.5.2. Rich club organization

The rich club organization is present in the brain network when the high-degree nodes are more massively interconnected than that expected by chance (van den Heuvel and Sporns, 2011). In brief, for a given unweighted network, rich-club organization is estimated by the rich-club coefficient Φ(k), which is defined as the ratio of connections between the subset of selected nodes and the number of possible maximized connections between them. That is, Φ(k) is given by:

$$\Phi(k) = \frac{2E_{>k}}{N_{>k}(N_{>k} - 1)}$$

where k is the number of connections of node i, $N_{>k}$ is the number of remaining nodes, and $E_{>k}$ is the number of remaining connections after removal of the nodes with connections less than k.

Meanwhile, we computed normalized rich-club coefficients $\Phi_{norm}(k)$ by averaging the rich-club coefficients over 1,000 random networks. The formal computational formula was described as below:

$$\Phi norm(k) = \frac{\Phi(k)}{\Phi_{random}(k)}$$

The normalized coefficient $\Phi_{norm}(k) > 1$ over a range of k indicated the existence of rich club organization in the brain network (Rubinov and Sporns, 2010; van den Heuvel and Sporns, 2011).

Rich club nodes were selected on the basis of the group-averaged functional network. The rich club nodes were defined as the top 19 (12%) brain regions with the highest average nodal degree of all regions in the group (van den Heuvel et al., 2013). Based on the categorization of the nodes into rich club nodes and non-rich club nodes, the edges of the functional network were classified into rich club connections, linking two rich club nodes; feeder connections, linking one rich club node to one non-rich club node; and local connections, linking non-rich club nodes (van den Heuvel and Sporns, 2011; van den Heuvel et al., 2013).

2.5.3. Modular architecture

The Dos-160 template divided the 160 ROIs into six modules (DMN, FPN, CON, SMN, ON and CN). We calculated the mean strength of intra- and inter-modular connections among MELAS-acute, MELAS-chronic and NC groups. For each subject, the mean strength of intra-module was the average number of intra-modular connections of the selected module, and the mean strength of the inter-module was the average number of inter-modular connections between the selected module and other modules.

2.6. Lesion probability map

Spatial distribution maps of stroke-like lesions (SLLs) were drawn to observe the relationship between SLLs and the properties of brain functional network in MELAS patients. Acute SLLs were defined as fresh ischemic-like lesions showing gyral swelling and subcortical white matter hyperintensity on FLAIR, and chronic SLLs were characterized by the areas of encephalomalacia, cortical thinning and hyperintensity on FLAIR (Ito et al., 2011). SLLs of each patient in MELAS-acute group and MELAS-chronic group were identified and manually segmented on FLAIR images slice by slice using the medical imaging interaction toolkit (MITK) software (http://www.mitk.org/wiki/MITK) (Nolden et al., 2013) by an experienced radiologist. SLLs mask images were then spatially normalized to standard MNI space. Using custom-written scripts in MATLAB, normalized and binarized SLLs maps were summed and averaged among all patients of each group to create the lesion probability maps for MELAS-acute and MELAS-chronic groups respectively.

2.7. Functional connectivity analysis

Functional connectivity (FC) was performed to investigate connectivity alterations between different modules and SLL regions using DPABI toolbox (Yan et al., 2016). Pearson correlation coefficients were calculated and transformed to Z values to obtain an approximate normal distribution.

2.8. Statistical analysis

Statistical analyses were performed using IBM SPSS software (version 23, Chicago, USA). One-way analysis of variance (ANOVA) test, chi-square test and Mann-Whitney *U* test were performed to analyse the group differences in the demographic and clinical data. P value < 0.05 was considered statistically significant.

For the network parameters (including global metrics, rich club organization and modular connections), we initially performed ANOVA non-parametric permutation test (10,000 times) to estimate the group effect among MELAS-acute, MELAS-chronic and NC groups. The 95th percentile of the null distribution was used as the significance threshold for cluster correction, corresponding to $p < 0.05$. The post hoc analyses were then implemented to determine the between-group differences using non-parametric permutation test (10,000 times) in a similar method for metrics with a significant group effect. To correct the multiple comparisons, the false discovery rate (FDR) correction was performed for each network parameter. The significance level for post hoc pairwise comparisons was set to FDR-corrected $p < 0.05$ across all pairs of groups. In addition, false positive correction for N-node statistical comparison was applied to correct the multiple comparisons for nodal parameters. This correction method has been used in many graph theory analyses, particularly for the comparisons of nodal metrics (Jung et al., 2017; Lynall et al., 2010; Meng et al., 2014; Wang et al., 2016, 2019b). The significance threshold was set to 1/(amount of nodes), meaning that nodes with $p < 0.00625$ (1/160) to be 'significant' in this study. Age and gender were used as nuisance covariates of no interest and regressed out throughout the entire analysis.

Pearson correlation coefficient was calculated to assess the correlations between SLL volumes and global network metrics (γ, λ, σ, Cp, Lp, E_{loc}, E_{glob}) in MELAS patients at acute stage and chronic stage, respectively. The significance level was set to P value < 0.05.

Receiver operating characteristic (ROC) curve was utilized to evaluate the possibility that rs-fMRI can be used as a tool to differentiate MELAS-acute group from MELAS-chronic group. The network parameters with significant between-group differences were extracted to perform ROC curve analysis. Area under the curve (AUC): 0.9–1.0 = excellent, 0.8–0.9 = good, 0.7–0.8 = fair, 0.6–0.7 = poor, and 0.5–0.6 = fail. The optimal cut-off point was determined by the corresponding maximized Youden's index J (J = sensitivity + specificity − 1).

2.9. Validation analysis

To ensure the same number of connections across all subjects, we used a single network sparsity (S = 15%) during the functional network construction. In order to determine whether our main results depended on the choice of network sparsity, we conducted analyses at two additional sparsity thresholds (S = 10% and S = 20%).

3. Results

3.1. Demographics and clinical data

There were no significant group differences in age, gender, age of disease onset and disease duration (all $p > 0.05$, Table 1). At acute stage, MELAS patients presented SLEs symptoms including seizure, headache, vomiting, aphasia, cortical blindness, hearing loss and motor weakness.

3.2. SLLs spatial distribution

The SLLs probability maps revealed that acute and chronic SLLs were

Table 1
Demographic and clinical characteristics of the participants.

Characteristics	MELAS-acute (n = 22)	MELAS-chronic (n = 23)	NC (n = 22)	p-value
Age (years)	25.7 ± 8.8	29.2 ± 11.3	29.1 ± 6.9	0.466 [a]
Gender (M/F)	12/10	12/11	10/12	0.925[b]
Age of disease onset (years)	25.7 ± 9.2	26.1 ± 10.4	–	0.521[c]
Disease duration (years)	2.4 ± 2.2	2.5 ± 1.8	–	0.641[c]
SLE symptoms (n, %)				
Seizure	15 (68%)	–	–	–
Headache	12 (55%)	–	–	–
Vomiting	10 (45%)	–	–	–
Cortical blindness	10 (45%)	–	–	–
Motor weakness	9 (41%)	–	–	–
Aphasia	7 (32%)	–	–	–
Hearing loss	6 (27%)	–	–	–
SLL volumes (mm^3)	45585 ± 32922	16412 ± 14533	–	<0.001 [d]

For continuous variables, data are expressed as the mean ± standard deviation. MELAS-acute, MELAS patients at acute stage; MELAS-chronic, MELAS patients at chronic stage; NC, normal controls; M, male; F, female.

[a] The p value for age was obtained by one-way analysis of variance.

[b] The p value for gender distribution was obtained by chi-square test.

[c] The p value for disease onset and duration was obtained by Mann-Whitney *U* test.

[d] The P value for SLL volumes was obtained by independent two-sample Student's *t* test.

mainly located in temporal, occipital and parietal lobes (Fig. 1b, d), with greater volumes of brain coverage in MELAS-acute group than MELAS-chronic group (Table 1). According to Dos-160 template, these SLLs regions overlapped with the nodes involving DMN, FPN, CON, SMN and ON modules (Fig. 1c, e). As displayed in Table 2, both MELAS-acute and MELAS-chronic groups showed the greatest overlap between ON module and SLL region (100% for acute group, 95% for chronic group).

3.3. Group differences in global and nodal metrics

Both MELAS patients and control subjects showed a small-world topology ($\gamma > 1$, $\lambda \approx 1$, $\sigma > 1$) of brain functional network. Among these three groups, significant group effects in global network metrics (γ, λ, σ, Cp, E_{loc}) were observed (Fig. 2). Post hoc comparisons showed reduced γ, λ, Cp and E_{loc} in both MELAS-acute and MELAS-chronic groups compared with NC. The acute patients also showed decreased σ relative to the controls. In addition, compared with MELAS-chronic group, MELAS-acute group showed reduced γ, λ, Cp and E_{loc} (all $p < 0.05$ with FDR-correction). In addition, there were no significant correlations between acute/chronic SLL volumes and global network metrics in MELAS patients (all $p > 0.05$).

Table 2
Overlap between SLL and modules in MELAS-acute and MELAS-chronic group.

Group	Module	Nodes in SLL	Total nodes in module	Overlap (%)
MELAS-acute				
	DMN	22	34	65
	FPN	8	21	38
	CON	10	32	31
	SMN	13	33	39
	ON	22	22	100
	CN	9	18	50
MELAS-chronic				
	DMN	10	34	29
	FPN	12	21	57
	CON	4	32	13
	SMN	1	33	3
	ON	21	22	95
	CN	3	18	17

SLL, stroke-like lesion; MELAS-acute, MELAS patients at acute stage; MELAS-chronic, MELAS patients at chronic stage; DMN: the default mode network; FPN: the fronto-parietal network; CON: the cingulo-opercular network; SMN: the sensorimotor network; ON: the occipital network; CN: the cerebellum network.

For nodal metrics, compared with NC, MELAS-acute and MELAS-chronic groups showed significantly decreased DC in 7 and 5 nodes, respectively, both involving CON and ON modules, and increased DC in 3 nodes (involving DMN and CON modules) and 1 node (involving DMN module) (Fig. 3a, b). Relative to MELAS-chronic group, MELAS-acute group exhibited significantly decreased DC in 2 nodes involving CON and CN modules (Fig. 3c). In addition, compared with NC, MELAS-acute group showed significantly lower E_{nodal} in 3 nodes involving CON and ON modules and higher E_{nodal} in 5 nodes involving DMN, FPN and CON modules, whereas MELAS-chronic group demonstrated significantly lower E_{nodal} in 3 nodes involving DMN, ON modules, and higher E_{nodal} in 4 nodes involving DMN, FPN, CON modules, respectively (Fig. 4a, b). Compared with MELAS-chronic group, MELAS-acute group exhibited significantly decreased E_{nodal} in 1 node involving CN module and increased E_{nodal} in 1 node involving DMN module (Fig. 4c). All of these nodes were listed in Tables S2 and S3 (supplementary materials).

3.4. Group differences in rich club organization

Fig. 5a illustrated the normalized rich club coefficient $\Phi_{norm}(k)$ for three groups over the range of degrees from DC = 1 to DC = 35. The characteristic rich club organization of functional network ($\Phi_{norm}(k) > 1$) was observed for both MELAS patients and controls. Compared with the controls, the acute patients demonstrated reduced $\Phi_{norm}(k)$ from DC = 28 to DC = 35; the chronic patients showed reduced $\Phi_{norm}(k)$ from DC = 30 to DC = 35. While, there was no significant difference of $\Phi_{norm}(k)$ between MELAS-acute and MELAS-chronic groups.

In addition, 19 rich club nodes were identified for each group. The distribution pattern of rich club nodes was relatively similar between MELAS-chronic and NC groups, but it was different from MELAS-acute group. (Fig. 5b, Table S4). In particularly, compared with NC group, the newly formed rich hub nodes in MELAS-acute group were mainly in DMN, while none rich hub nodes were found in ON. Moreover, we found that mean strength of rich club connections was significant lower in both MELAS-acute and MELAS-chronic groups than that in NC group ($p < 0.05$ with FDR-correction) (Fig. 5d). No significant group differences were observed in mean strength of feeder and local connections.

3.5. Group differences in intra- and inter-modular connections

Fig. 6 showed the mean strength of 6 intra-modular and 15 inter-modular connections for each group. Significant group differences were found in 1 intra-modular connection and 5 inter-modular connections. Post hoc analysis revealed that the two MELAS groups exhibited similar changes of modular connections in ON, ON-CN DMN-SMN, FPN-SMN and FPN-ON as compared with NC group. When compared with MELAS-chronic group, MELAS-acute group showed decreased connection strength in ON, ON-CN and increased connection strength in DMN-SMN, FPN-SMN (all $p < 0.05$ with FDR-correction).

3.6. ROC analysis for differentiating MELAS-acute from MELAS-chronic

As displayed in Table 3, the ROC analysis demonstrated that most of network parameters showed fair performances (AUC = 0.7–0.8, $p < 0.05$) in differentiating MELAS-acute from MELAS-chronic.

3.7. FC between SLL and modules in MELAS-acute and MELAS-chronic groups

We found that both MELAS-acute and MELAS-chronic groups exhibited the strongest FC between the lesion and the ON module (Fig. S1).

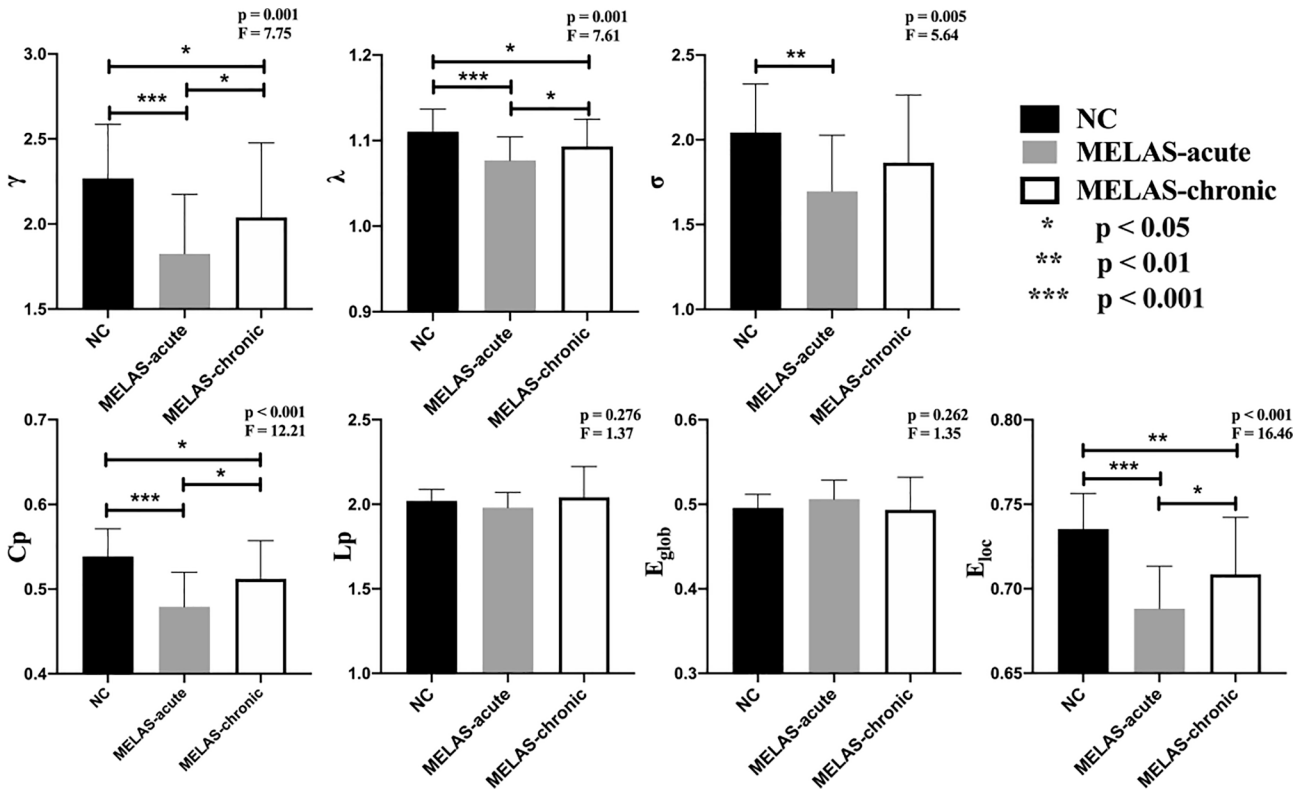

Fig. 2. The differences in global metrics of the brain functional networks among MELAS-acute, MELAS-chronic and NC groups. γ, normalized clustering coefficient; λ, normalized characteristic path length; δ = λ/γ, small-world characteristic; Cp, clustering coefficient; Lp, shortest path length; E_{glob}, global efficiency; E_{loc}, local efficiency. All of the significance levels were set to $p < 0.05$ with the FDR correction.

3.8. Validation results under different network sparsity thresholds

We found that most of our findings were highly reproducible under different network sparsity thresholds (S = 10% and S = 20%) (Table S5 and Fig. S2). Specifically, small-worldness and rich club organization were still demonstrated in MELAS-acute, MELAS-chronic and NC groups. For the global metrics, MELAS patients consistently showed significantly lower γ, Cp and E_{loc} compared with the controls. For the intra- and inter-modular connections, MELAS patients also exhibited abnormal connection strength in ON, DMN-SMN, FPN-SMN, FPN-CN and ON-CN.

4. Discussion

In this study, we constructed whole-brain functional network for MELAS patients and control subjects based on graph theory. To our knowledge, this is the first study to investigate the alterations of topological organization in MELAS patients at acute and chronic stages. Overall, small-world topology of functional network was exhibited in both MELAS patients and control subjects. However, compared with the controls, MELAS patients (especially at acute stage) showed (1) decreased global metrics (γ, Cp and E_{loc}); (2) abnormal nodal parameters (DC and E_{nodal}) mainly in DMN, CON and ON modules; (3) disrupted rich club organization with reduced $\Phi_{norm}(k)$ and rich club connections; (4) altered intra- and inter-modular connections mainly in ON, DMN-SMN, FPN-SMN, FPN-CN and ON-CN modules.

There are three types of networks in the framework of graph theory: regular, small-world and random. The small-world network combines the advantages of regular and random networks, which means that it supports high efficiency of both specialized processing in local regions and integrated processing over the global network (Bassett and Bullmore, 2017). Generally, the human brain is believed to be a very complex and largely interconnected network with small-world attribute (Rubinov and Sporns, 2010; Sporns, 2011). In this study, we observed that all of healthy subjects and MELAS patients at acute and chronic stages exhibited efficient and economic small-world topology, as reflected by $\gamma > 1$, $\lambda \approx 1$ and $\sigma > 1$.

However, at the global level, significantly lower γ, λ, Cp and E_{loc} were found in MELAS groups as compared with NC group, and the effect was more significant in MELAS-acute group. In addition, these global network metrics were not correlated with acute/chronic SLL volumes in MELAS. The results indicated that the disrupted balance between functional segregation and integration existed in MELAS patients, which was independent of SLL volumes. Specifically, the disrupted functional segregation (decreased γ, Cp and E_{loc}) in MELAS patients suggested a limited ability of segregating information flow for specialized processing regionally. While the improved functional integration (decreased λ) in MELAS patients implied high efficiency for global information communication. Taken together, MELAS patients (especially at acute stage) demonstrated topological disturbance and reorganization of the whole brain. Similar findings can be found in other diseases, such as bipolar disorder (Wang et al., 2019b), schizophrenia (Wang et al., 2019a) and ischemic stroke (Bournonville et al., 2018).

Turning to the nodal level, there were several nodes with abnormal degree centrality or nodal efficiency in MELAS patients compared with the controls, indicating nodal reorganization in whole-brain functional network. Among these abnormal nodes, we noted that the nodes showing both decreased degree centrality and nodal efficiency in MELAS patients were mainly in ON module. Degree centrality is a measure of node importance in the network, and nodal efficiency is an index that evaluates the capacity of a node for information communication (Liao et al., 2017). Meanwhile, the ON is thought to be related to visual system (Yeo et al., 2011). Our result suggested that these abnormal nodes in ON may have reduced connectivity and efficiency for the communication with other regions. Therefore, the visual function deficit in MELAS patients is most likely a consequence of network disruption. In addition,

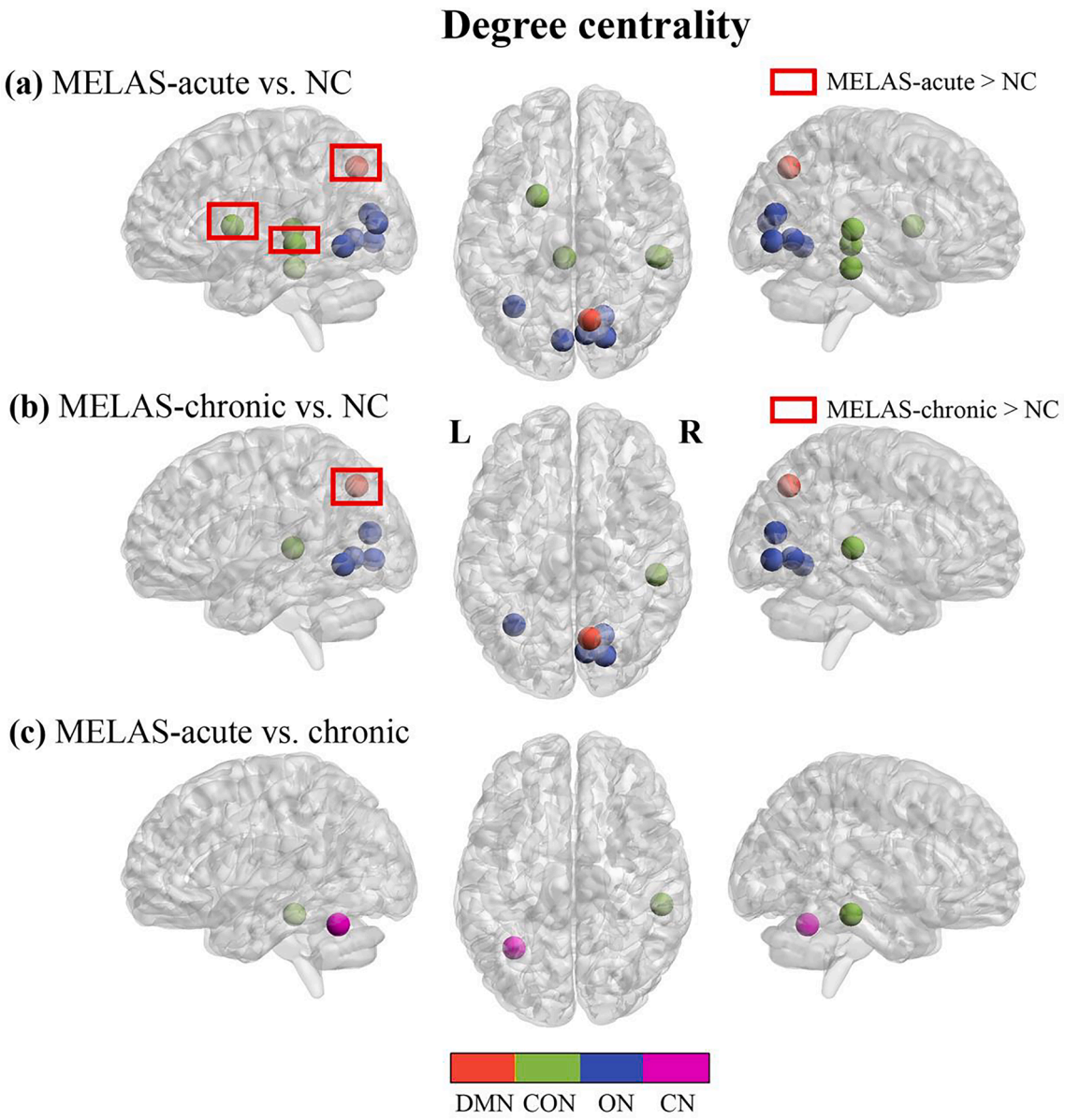

Fig. 3. Nodes with abnormal degree centrality in brain functional networks for the comparisons of MELAS-acute vs NC (a), MELAS-chronic vs. NC (b) and MELAS-acute vs. MELAS-chronic (c). DMN: the default mode network; CON: the cingulo-opercular network; ON: the occipital network; CN: the cerebellum network. The nodes were listed in Table S2.

the node of precuneus in DMN module showed both increased degree centrality and nodal efficiency in MELAS patients as compared with NC. The precuneus, a central core of DMN, is associated with motor, visual and cognitive functions (Bruner et al., 2017; Luo et al., 2019). Our result provided evidence that precuneus played an important role as a compensatory node to keep efficient information communication across the functional network in MELAS.

In our study, both MELAS patients and healthy controls showed a rich club organization. In other words, all subjects had highly connected nodes that were more interconnected than would be expected by chance (van den Heuvel and Sporns, 2011). Despite the presence of a rich club organization, MELAS patients showed a significant reduction in normalized rich-club coefficient compared with healthy controls. The result indicated that, given the biological cost, it was difficult for MELAS patients to maintain or repair the core network. In addition, after identifying the rich club nodes for each group, the distribution pattern of rich club nodes was relatively similar between MELAS-chronic and NC groups, but it was different from MELAS-acute group. It meant that the architecture of rich club nodes was reorganized during acute stage. It is worthy to note that, compared with NC group, the newly formed rich hub nodes in MELAS-acute group were mainly in DMN, while none rich hub nodes were found in ON. That was to say, for MELAS patients at acute stage, the change of the nodes in DMN from non-rich club to rich club was a functional reorganization to compensate for the dysfunction of the nodes in ON. Furthermore, it has been proposed that the connections among rich club nodes are central to information integration among different subsystems of human brain (van den Heuvel and Sporns, 2011; van den Heuvel et al., 2013). In this study, we found decreased rich club connectivity in MELAS patients compared with the controls. It suggested that the rich club connections among the hub regions, acted as a central high cost and high capacity backbone for global brain communication (van den Heuvel et al., 2012), were prone to be disrupted in MELAS patients.

Modular architecture is an optimized organization in the brain network that combines functional specialization and integration to enable a balance between energy cost and communication efficiency

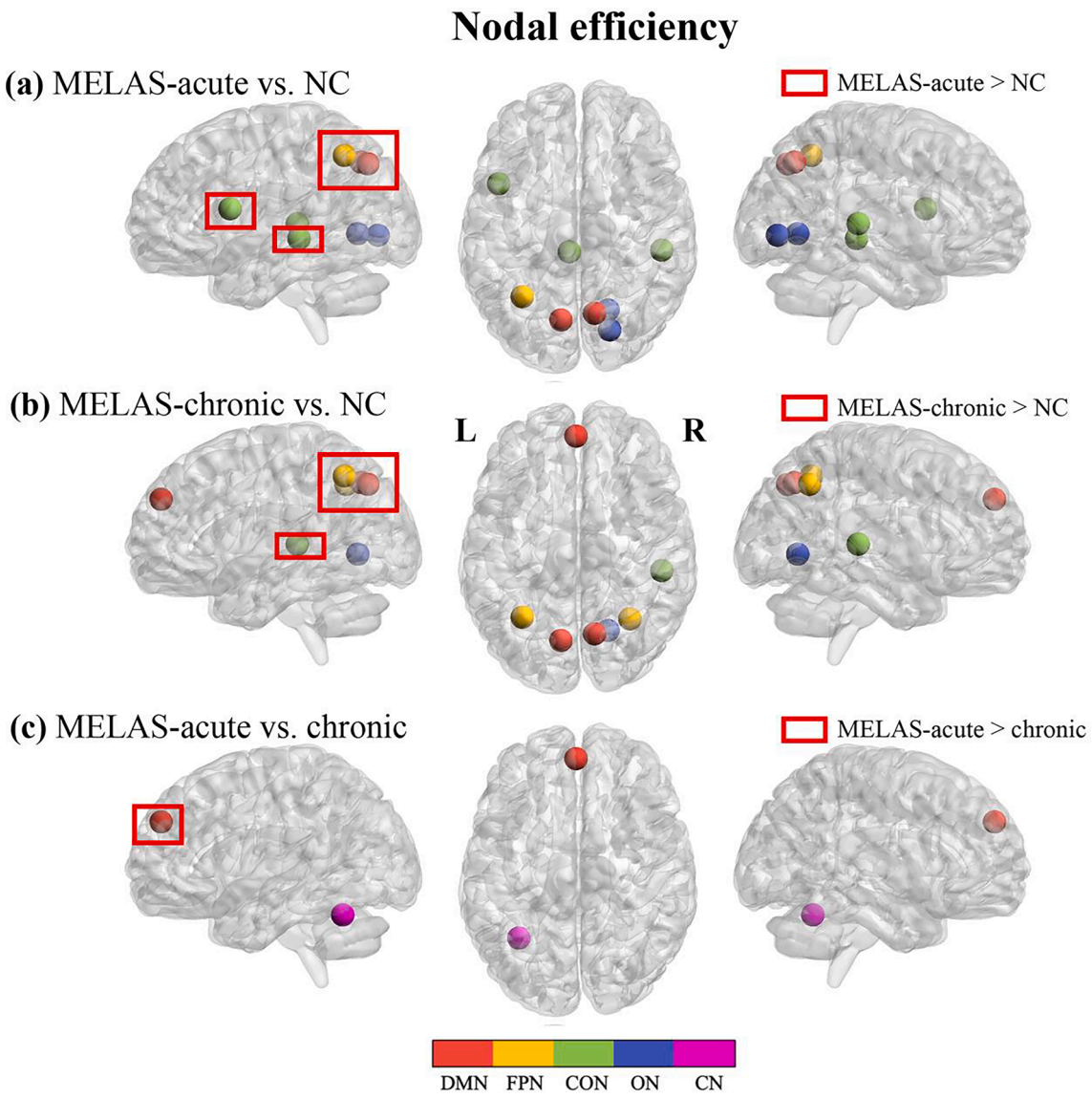

Fig. 4. Nodes with abnormal nodal efficiency in brain functional networks for the comparisons of MELAS-acute vs NC (a), MELAS-chronic vs. NC (b) and MELAS-acute vs. MELAS-chronic (c). DMN: the default mode network; FPN: the fronto-parietal network; CON: the cingulo-opercular network; ON: the occipital network; CN: the cerebellum network. The nodes were listed in Table S3.

(Sporns and Betzel, 2016). In present study, except the inter-module connection between PFN and CN in acute group, shared alterations of intra- and inter-modular connections were observed in the two patient groups compared with control subjects. To be specific, decreased intra-module connectivity was revealed in the ON in MELAS patients. The ON consists of visual cortex and is associated with visual function (Yeo et al., 2011). Thus, the hypoconnectivity within this module may explain the frequent clinical presentations with cortical blindness or hemianopia in MELAS patients, especially during acute stage (Bhatia et al., 2020; Ito et al., 2011; Yatsuga et al., 2012). In addition, decreased inter-modular connectivity was found in ON-CN, while increased inter-modular connectivity was detected in DMN-SMN, FPN-ON and FPN-SMN in MELAS patients. As we known, the ON, SMN and CN play important roles in visual-sensor and motor-sensor functions, respectively (Fine et al., 2002; Hardwick et al., 2013; Niemeier et al., 2005). Meanwhile, the DMN and SMN are higher-order modules that support a wide range of cognitive and attention functions for stimuli and responses (Corbetta and Shulman, 2002; Raichle, 2015). Collectively, the alterations of inter-modular connections in this study implied that MELAS patients might have inappropriate integration between bottom-up sensory input and top-down regulation, which was more obvious in acute group.

Moreover, both MELAS-acute and MELAS-chronic groups showed the greatest overlap and strongest FC between ON module and SLL region. As a result, for MELAS patients, the changes of degree centrality, rich club nodes and intra-modular connection in ON module may be associated with the effect of SLL. Specifically, compared with the control group, the degree centrality and intra-module connection of ON module in MELAS groups were significantly decreased. In addition, there were no rich club nodes in ON module for MELAS groups. Based on above evidences, we believed that the SLL may affect the topological organization of corresponding brain regions in MELAS patients. Furthermore, results of ROC analysis showed that several network parameters had fair performances in distinguishing MELAS patients at acute stage from chronic stage. Notably, the intra-module connection of ON module showed 78.26% predictive accuracy. Therefore, it implied that ON is an important hub in MELAS and the parameters of graph theory analysis may be used as biomarkers for predicting the clinical outcome of MELAS.

This study had several limitations. First, there is no widely accepted optimal approach for defining nodes and edges. We used the Dos-160

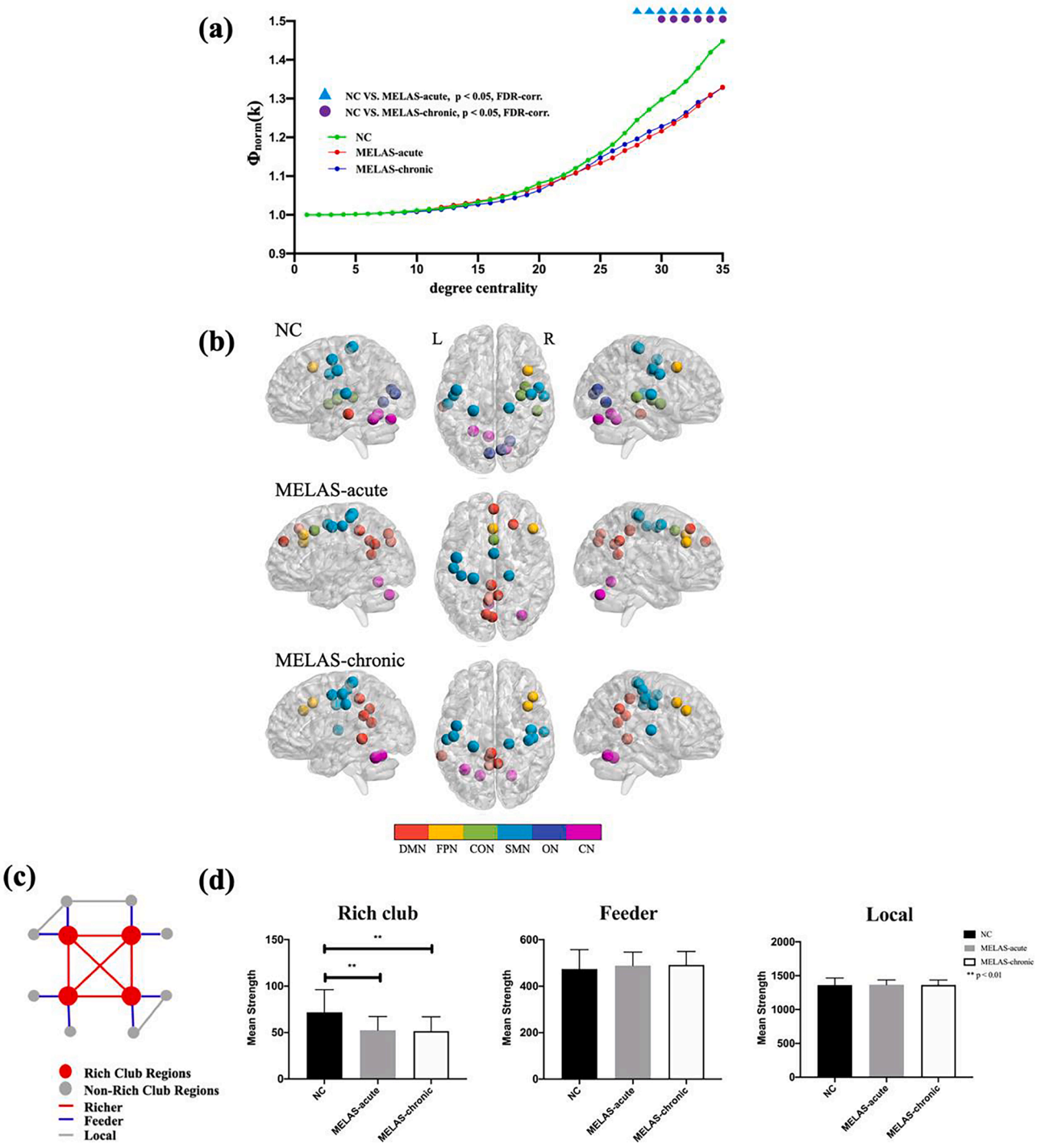

Fig. 5. The rich club organization for MELAS-acute, MELAS-chronic and NC groups. The normalized rich club coefficient curve and between-group differences under a series of thresholds degree centrality (a). The distribution of rich club nodes in the whole brain for each group (b). The nodes were listed in Table S4. The colors of nodes represented the different modules of brain functional networks according to Dos-160 template. DMN: the default mode network; FPN: the fronto-parietal network; CON: the cingulo-opercular network; SMN: the sensorimotor network; ON: the occipital network; CN: the cerebellum network. A simplified example of the three classes of connections: rich club connections, linking two rich club nodes; feeder connections, linking one rich club node to one non-rich club node; and local connections, linking two non-rich club nodes (c). Group differences in the mean strength of the rich-club, feeder and local connections (d).

template and binarized matrix in the construction of graphs. Other construction strategies (including different brain template and weighted network model) should be considered to verify the repeatability of our results. Second, behavioral assessments were not acquired in this study, and future research in MELAS should combine rs-fMRI results with cognitive or psychological tests to better explain how the observed effects in network topology relate to behavioral changes. Finally, future longitudinal studies, instead of cross-sectional studies, would better delineate the changes of brain connectomes between acute and chronic stages.

5. Conclusions

In summary, MELAS patients, especially those at acute stage,

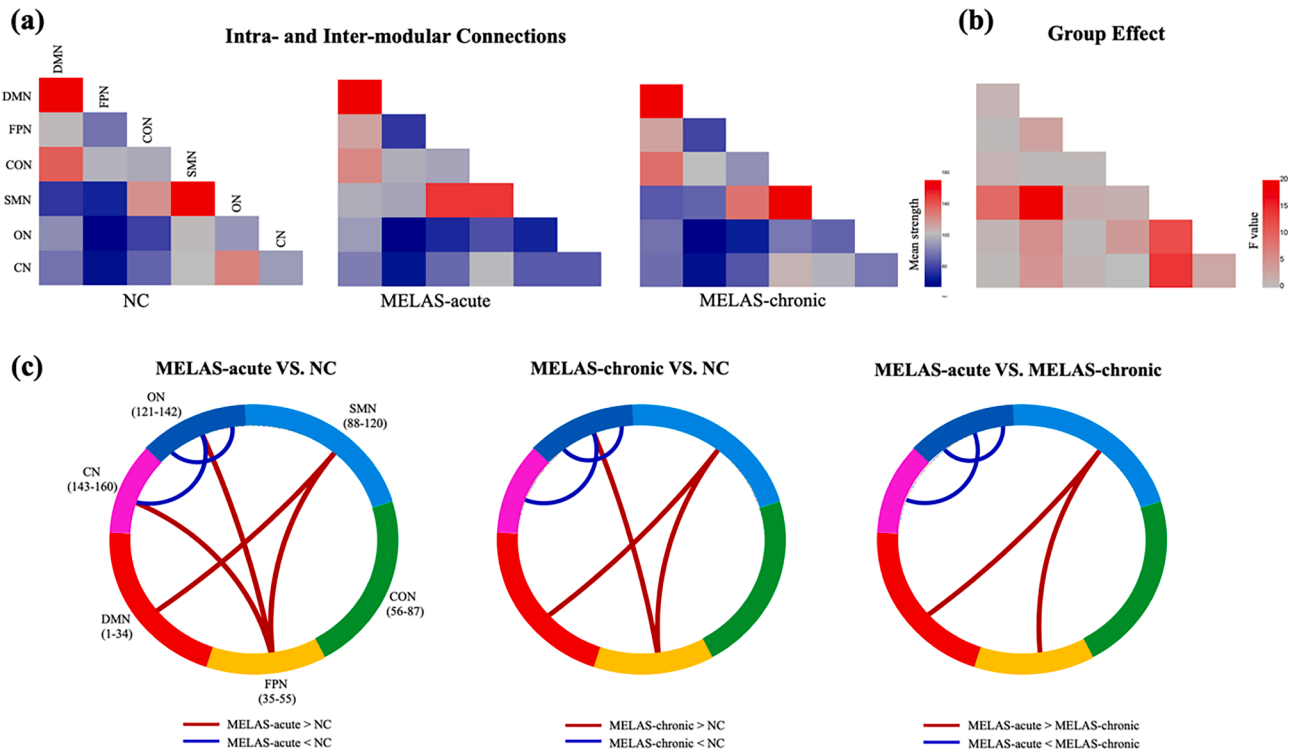

Fig. 6. The matrices showed mean strength of intra- and inter-modular connections for MELAS-acute, MELAS-chronic and NC groups (a). The matrix illustrated the group effects among the three groups (b). Between-group differences of intra- and inter-modular connections for each pair of groups (c). Red and blue lines represented significantly more connections and fewer connections, respectively. DMN: the default mode network; FPN: the fronto-parietal network; CON: the cingulo-opercular network; SMN: the sensorimotor network; ON: the occipital network; CN: the cerebellum network. (For interpretation of the references to color in this figure legend, the reader is referred to the web version of this article.)

Table 3
ROC analysis in network parameters showing significant differences between MELAS-acute and MELAS-chronic groups.

Parameters	ROC curve			
	AUC (%)	Sensitivity (%)	Specificity (%)	p-value
Global metrics				
γ	67.59	52.17	86.36	0.043
λ	67.39	43.48	86.36	0.045
Cp	70.16	39.13	90.91	0.021
E_{loc}	67.79	52.17	81.82	0.041
Degree centrality				
fusiform	75.10	65.22	81.82	0.004
lat cerebellum	79.64	78.26	77.27	<0.001
Nodal efficiency				
mPFC	74.41	69.57	68.18	0.005
lat cerebellum	75.10	60.87	86.36	0.004
Intra-modular				
ON	78.26	82.61	68.18	0.001
Inter-modular				
ON-CN	75.69	86.96	59.09	0.003
DMN-SMN	71.54	52.17	77.27	0.001
FPN-SMN	68.48	43.48	86.36	0.034

γ, normalized clustering coefficient; λ, normalized characteristic path length; Cp, clustering coefficient; E_{loc}, local efficiency; DMN: the default mode network; FPN: the fronto-parietal network; SMN: the sensorimotor network; ON: the occipital network; CN: the cerebellum network.

exhibited topological reorganization of whole-brain functional network, with alterations of global and nodal metrics, rich club organization and modular connections. In addition, network abnormalities in MELAS patients appeared to be affected by the effects of stroke-like lesions. In addition, graph theory analysis based on rs-fMRI may play a role in monitoring the disease status and predicting the clinical outcome for MELAS.

Funding

This study was supported by the Science and Technology Commission of Shanghai Municipality (19411951200, 19ZR1407900, 20S31904300).

CRediT authorship contribution statement

Rong Wang: Investigation, Methodology, Validation, Formal analysis, Writing - original draft, Formal analysis. **Jie Lin:** Investigation, Methodology, Resources, Conceptualization. **Chong Sun:** Investigation, Methodology, Resources. **Bin Hu:** Investigation, Resources. **Xueling Liu:** Investigation, Resources. **Daoying Geng:** Project administration, Funding acquisition. **Yuxin Li:** Investigation, Methodology, Conceptualization, Methodology, Writing - review & editing, Supervision, Project administration, Funding acquisition. **Liqin Yang:** Investigation, Methodology, Formal analysis, Writing - review & editing, Supervision, Funding acquisition.

Declaration of Competing Interest

The authors declare that they have no known competing financial interests or personal relationships that could have appeared to influence the work reported in this paper.

Appendix A. Supplementary data

Supplementary data to this article can be found online at https://doi.org/10.1016/j.nicl.2020.102480.

References

Adhikari, M.H., Hacker, C.D., Siegel, J.S., Griffa, A., Hagmann, P., Deco, G., Corbetta, M., 2017. Decreased integration and information capacity in stroke measured by whole brain models of resting state activity. Brain 140, 1068–1085.

Aerts, H., Fias, W., Caeyenberghs, K., Marinazzo, D., 2016. Brain networks under attack: robustness properties and the impact of lesions. Brain 139 (12), 3063–3083. https://doi.org/10.1093/brain/aww194.

Albert, K.M., Potter, G.G., Boyd, B.D., Kang, H., Taylor, W.D., 2019. Brain network functional connectivity and cognitive performance in major depressive disorder. J. Psychiatr. Res. 110, 51–56. https://doi.org/10.1016/j.jpsychires.2018.11.020.

Bassett, D.S., Bullmore, E.T., 2017. Small-world brain networks revisited. Neuroscientist 23 (5), 499–516. https://doi.org/10.1177/1073858416667720.

Bhatia, K.D., Krishnan, P., Kortman, H., Klostranec, J., Krings, T., 2020. Acute cortical lesions in MELAS syndrome: anatomic distribution, symmetry, and evolution. AJNR Am. J. Neuroradiol. 41, 167–173.

Biswal, B., Zerrin Yetkin, F., Haughton, V.M., Hyde, J.S., 1995. Functional connectivity in the motor cortex of resting human brain using echo-planar MRI. Magn. Reson. Med. 34 (4), 537–541. https://doi.org/10.1002/mrm.1910340409.

Bournonville, C., Hénon, H., Dondaine, T., Delmaire, C., Bombois, S., Mendyk, A.-M., Cordonnier, C., Moulin, S., Leclerc, X., Bordet, R., Lopes, R., 2018. Identification of a specific functional network altered in poststroke cognitive impairment. Neurology 90 (21), e1879–e1888. https://doi.org/10.1212/WNL.0000000000005553.

Bruner, E., Preuss, T.M., Chen, X.u., Rilling, J.K., 2017. Evidence for expansion of the precuneus in human evolution. Brain Struct. Funct. 222 (2), 1053–1060. https://doi.org/10.1007/s00429-015-1172-y.

Bullmore, E.d., Sporns, O., 2009. Complex brain networks: graph theoretical analysis of structural and functional systems. Nat. Rev. Neurosci. 10 (3), 186–198. https://doi.org/10.1038/nrn2575.

Corbetta, M., Shulman, G.L., 2002. Control of goal-directed and stimulus-driven attention in the brain. Nat. Rev. Neurosci. 3, 201–215.

Dai, Z., Lin, Q., Li, T., Wang, X., Yuan, H., Yu, X., He, Y., Wang, H., 2019. Disrupted structural and functional brain networks in Alzheimer's disease. Neurobiol. Aging 75, 71–82.

Dosenbach, N.U., Nardos, B., Cohen, A.L., Fair, D.A., Power, J.D., Church, J.A., Nelson, S. M., Wig, G.S., Vogel, A.C., Lessov-Schlaggar, C.N., Barnes, K.A., Dubis, J.W., Feczko, E., Coalson, R.S., Pruett Jr., J.R., Barch, D.M., Petersen, S.E., Schlaggar, B.L., 2010. Prediction of individual brain maturity using fMRI. Science (New York N.Y.) 329, 1358–1361.

El-Hattab, A.W., Adesina, A.M., Jones, J., Scaglia, F., 2015. MELAS syndrome: clinical manifestations, pathogenesis, and treatment options. Mol. Genet. Metab. 116, 4–12.

Fine, E.J., Ionita, C.C., Lohr, L., 2002. The history of the development of the cerebellar examination. Semin. Neurol. 22, 375–384.

Fox, M.D., Zhang, D., Snyder, A.Z., Raichle, M.E., 2009. The global signal and observed anticorrelated resting state brain networks. J. Neurophysiol. 101, 3270–3283.

Friston, K.J., Williams, S., Howard, R., Frackowiak, R.S., Turner, R., 1996. Movement-related effects in fMRI time-series. Magn. Reson. Med. 35, 346–355.

Goto, Y., Nonaka, I., Horai, S., 1990. A mutation in the tRNA(Leu)(UUR) gene associated with the MELAS subgroup of mitochondrial encephalomyopathies. Nature 348, 651–653.

Göttlich, M., Münte, T.F., Heldmann, M., Kasten, M., Hagenah, J., Krämer, U.M., 2013. Altered resting state brain networks in Parkinson's disease. PLoS ONE 8, e77336.

Hardwick, R.M., Rottschy, C., Miall, R.C., Eickhoff, S.B., 2013. A quantitative meta-analysis and review of motor learning in the human brain. Neuroimage 67, 283–297.

He, Y., Evans, A., 2010. Graph theoretical modeling of brain connectivity. Curr. Opin. Neurol. 23, 341–350.

Hongo, Y., Kaneko, J., Suga, H., Ishima, D., Kitamura, E., Akutsu, T., Onozawa, Y., Kanazawa, N., Goto, T., Nishiyama, K., Iizuka, T., 2019. A cluster of disseminated small cortical lesions in MELAS: its distinctive clinical and neuroimaging features. J. Neurol. 266, 1459–1472.

Iizuka, T., Sakai, F., Suzuki, N., Hata, T., Tsukahara, S., Fukuda, M., Takiyama, Y., 2002. Neuronal hyperexcitability in stroke-like episodes of MELAS syndrome. Neurology 59, 816–824.

Ito, H., Mori, K., Kagami, S., 2011. Neuroimaging of stroke-like episodes in MELAS. Brain Dev. 33, 283–288.

Jung, W.H., Yücel, M., Yun, J.Y., Yoon, Y.B., Cho, K.I., Parkes, L., Kim, S.N., Kwon, J.S., 2017. Altered functional network architecture in orbitofronto-striato-thalamic circuit of unmedicated patients with obsessive-compulsive disorder. Hum. Brain Mapp. 38, 109–119.

Kaufmann, P., Engelstad, K., Wei, Y., Kulikova, R., Oskoui, M., Sproule, D.M., Battista, V., Koenigsberger, D.Y., Pascual, J.M., Shanske, S., Sano, M., Mao, X., Hirano, M., Shungu, D.C., Dimauro, S., De Vivo, D.C., 2011. Natural history of MELAS associated with mitochondrial DNA m.3243A>G genotype. Neurology 77, 1965–1971.

Koenig, M.K., Emrick, L., Karaa, A., Korson, M., Scaglia, F., Parikh, S., Goldstein, A., 2016. Recommendations for the management of strokelike episodes in patients with mitochondrial encephalomyopathy, lactic acidosis, and strokelike episodes. JAMA Neurol. 73, 591–594.

Lee, H.N., Yoon, C.S., Lee, Y.M., 2018. Correlation of serum biomarkers and magnetic resonance spectroscopy in monitoring disease progression in patients with mitochondrial encephalomyopathy, lactic acidosis, and stroke-like episodes due to mtDNA A3243G mutation. Front. Neurol. 9, 621.

Li, Y., Xu, W., Sun, C., Lin, J., Qu, J., Cao, J., Li, H., Yang, L., 2019. Reversible dilation of cerebral macrovascular changes in MELAS episodes. Clin. Neuroradiol. 29, 321–329.

Liao, X., Vasilakos, A.V., He, Y., 2017. Small-world human brain networks: perspectives and challenges. Neurosci. Biobehav. Rev. 77, 286–300.

Luo, Z., Zeng, L.L., Qin, J., Hou, C., Shen, H., Hu, D., 2019. Functional parcellation of human brain precuneus using density-based clustering. Cereb. Cortex.

Lynall, M.E., Bassett, D.S., Kerwin, R., McKenna, P.J., Kitzbichler, M., Muller, U., Bullmore, E., 2010. Functional connectivity and brain networks in schizophrenia. J. Neurosci. 30, 9477–9487.

Malhotra, K., Liebeskind, D.S., 2016. Imaging of MELAS. Curr. Pain Headache Rep. 20, 54.

Meng, C., Brandl, F., Tahmasian, M., Shao, J., Manoliu, A., Scherr, M., Schwerthöffer, D., Bäuml, J., Förstl, H., Zimmer, C., Wohlschläger, A.M., Riedl, V., Sorg, C., 2014. Aberrant topology of striatum's connectivity is associated with the number of episodes in depression. Brain 137, 598–609.

Murphy, K., Birn, R.M., Handwerker, D.A., Jones, T.B., Bandettini, P.A., 2009. The impact of global signal regression on resting state correlations: are anti-correlated networks introduced? Neuroimage 44, 893–905.

Niemeier, M., Goltz, H.C., Kuchinad, A., Tweed, D.B., Vilis, T., 2005. A contralateral preference in the lateral occipital area: sensory and attentional mechanisms. Cereb. Cortex 15, 325–331.

Nolden, M., Zelzer, S., Seitel, A., Wald, D., Müller, M., Franz, A.M., Maleike, D., Fangerau, M., Baumhauer, M., Maier-Hein, L., Maier-Hein, K.H., Meinzer, H.-P., Wolf, I., 2013. The medical imaging interaction Toolkit: challenges and advances: 10 years of open-source development. Int. J. Comput. Assist. Radiol. Surg. 8, 607–620.

Pavlakis, S.G., Phillips, P.C., DiMauro, S., De Vivo, D.C., Rowland, L.P., 1984. Mitochondrial myopathy, encephalopathy, lactic acidosis, and strokelike episodes: a distinctive clinical syndrome. Ann. Neurol. 16, 481–488.

Power, J.D., Mitra, A., Laumann, T.O., Snyder, A.Z., Schlaggar, B.L., Petersen, S.E., 2014. Methods to detect, characterize, and remove motion artifact in resting state fMRI. Neuroimage 84, 320–341.

Raichle, M.E., 2015. The brain's default mode network. Annu. Rev. Neurosci. 38, 433–447.

Rubinov, M., Sporns, O., 2010. Complex network measures of brain connectivity: uses and interpretations. Neuroimage 52, 1059–1069.

Sporns, O., 2011. The human connectome: a complex network. Ann. N. Y. Acad. Sci. 1224, 109–125.

Sporns, O., Betzel, R.F., 2016. Modular brain networks. Annu. Rev. Psychol. 67, 613–640.

Sudre, G., Choudhuri, S., Szekely, E., Bonner, T., Goduni, E., Sharp, W., Shaw, P., 2017. Estimating the heritability of structural and functional brain connectivity in families affected by attention-deficit/hyperactivity disorder. JAMA Psychiatr. 74, 76–84.

Syan, S.K., Smith, M., Frey, B.N., Remtulla, R., Kapczinski, F., Hall, G.B.C., Minuzzi, L., 2018. Resting-state functional connectivity in individuals with bipolar disorder during clinical remission: a systematic review. J. Psychiatr. Neurosci. 43, 298–316.

Tijms, B.M., Wink, A.M., de Haan, W., van der Flier, W.M., Stam, C.J., Scheltens, P., Barkhof, F., 2013. Alzheimer's disease: connecting findings from graph theoretical studies of brain networks. Neurobiol. Aging 34, 2023–2036.

Uehara, T., Yamasaki, T., Okamoto, T., Koike, T., Kan, S., Miyauchi, S., Kira, J., Tobimatsu, S., 2014. Efficiency of a "small-world" brain network depends on consciousness level: a resting-state FMRI study. Cereb. Cortex 24, 1529–1539.

van den Heuvel, M.P., Kahn, R.S., Goñi, J., Sporns, O., 2012. High-cost, high-capacity backbone for global brain communication. Proc. Natl. Acad. Sci. USA 109, 11372–11377.

van den Heuvel, M.P., Sporns, O., 2011. Rich-club organization of the human connectome. J. Neurosci. 31, 15775–15786.

van den Heuvel, M.P., Sporns, O., Collin, G., Scheewe, T., Mandl, R.C., Cahn, W., Goñi, J., Hulshoff Pol, H.E., Kahn, R.S., 2013. Abnormal rich club organization and functional brain dynamics in schizophrenia. JAMA Psychiatr. 70, 783–792.

Wang, J., Lu, M., Fan, Y., Wen, X., Zhang, R., Wang, B., Ma, Q., Song, Z., He, Y., Wang, J., Huang, R., 2016. Exploring brain functional plasticity in world class gymnasts: a network analysis. Brain Struct. Funct. 221, 3503–3519.

Wang, J., Wang, X., Xia, M., Liao, X., Evans, A., He, Y., 2015. GRETNA: a graph theoretical network analysis toolbox for imaging connectomics. Front. Hum. Neurosci. 9, 386.

Wang, L.X., Guo, F., Zhu, Y.Q., Wang, H.N., Liu, W.M., Li, C., Wang, X.R., Cui, L.B., Xi, Y. B., Yin, H., 2019a. Effect of second-generation antipsychotics on brain network topology in first-episode schizophrenia: a longitudinal rs-fMRI study. Schizophr. Res. 208, 160–166.

Wang, Y., Deng, F., Jia, Y., Wang, J., Zhong, S., Huang, H., Chen, L., Chen, G., Hu, H., Huang, L., Huang, R., 2019b. Disrupted rich club organization and structural brain connectome in unmedicated bipolar disorder. Psychol. Med. 49, 510–518.

Weissenbacher, A., Kasess, C., Gerstl, F., Lanzenberger, R., Moser, E., Windischberger, C., 2009. Correlations and anticorrelations in resting-state functional connectivity MRI: a quantitative comparison of preprocessing strategies. Neuroimage 47, 1408–1416.

Xia, M., Wang, J., He, Y., 2013. BrainNet Viewer: a network visualization tool for human brain connectomics. PLoS ONE 8, e68910.

Xu, W., Wen, J., Sun, C., Cao, J., Li, Y., Geng, D., 2018. Conventional and diffusional magnetic resonance imaging features of mitochondrial encephalomyopathy, lactic acidosis, and stroke-like episodes in Chinese patients: a study of 40 cases. J. Comput. Assist. Tomogr. 42, 510–516.

Yan, C.G., Wang, X.D., Zuo, X.N., Zang, Y.F., 2016. DPABI: Data processing & analysis for (resting-state) brain imaging. Neuroinformatics 14, 339–351.

Yang, G.J., Murray, J.D., Repovs, G., Cole, M.W., Savic, A., Glasser, M.F., Pittenger, C., Krystal, J.H., Wang, X.J., Pearlson, G.D., Glahn, D.C., Anticevic, A., 2014. Altered global brain signal in schizophrenia. Proc. Natl. Acad. Sci. USA 111, 7438–7443.

Yao, Z., Hu, B., Xie, Y., Moore, P., Zheng, J., 2015. A review of structural and functional brain networks: small world and atlas. Brain Inform. 2, 45–52.
Yatsuga, S., Povalko, N., Nishioka, J., Katayama, K., Kakimoto, N., Matsuishi, T., Kakuma, T., Koga, Y., 2012. MELAS: a nationwide prospective cohort study of 96 patients in Japan. BBA 1820, 619–624.
Yeo, B.T., Krienen, F.M., Sepulcre, J., Sabuncu, M.R., Lashkari, D., Hollinshead, M., Roffman, J.L., Smoller, J.W., Zöllei, L., Polimeni, J.R., Fischl, B., Liu, H., Buckner, R. L., 2011. The organization of the human cerebral cortex estimated by intrinsic functional connectivity. J. Neurophysiol. 106, 1125–1165.